

Doppler Radar-based Human Breathing Patterns Classification Using Support Vector Machine

Dongyu Miao, Heng Zhao, Hong Hong and Xiaohua Zhu

School of Electronic and Optical Engineering
Nanjing University of Science and Technology
Nanjing, People's Republic of China
hognju@njust.edu.cn

Changzhi Li

Department of Electrical and Computer Engineering
Texas Tech University
Lubbock, TX 79409, USA
changzhi.li@ttu.edu

Abstract—Monitoring and recognizing human breathing patterns is of great importance in preliminary disease diagnosis. This paper presents a noncontact human breathing patterns classification method based on the Doppler radar. The proposed classification method can be suitable for discriminating the breathing patterns automatically. The Support Vector Machine (SVM) classifier, which solves the nonlinear problem using kernel function, is widely used in pattern recognition. It is selected to classify four typical breathing patterns. Three features from the time-domain and short-term energy-domain are extracted for the classification. In the experiment, the SVM classifiers with six different kernel functions have been tested on a dataset of 60 samples from five healthy subjects. Through the 10-fold cross-validation, experimental results show that the cubic SVM classifier has the best classification accuracy rate of 93.3%.

Keywords—Doppler radar; breathing pattern; feature extraction; SVM classifier

I. INTRODUCTION

It is known that respiration is one of the most important vital signs of human body. Breathing patterns can directly indicate health conditions. Abnormal breathing is usually accompanied by certain diseases such as stroke, brain tumor, and metabolic acidosis [1]. Sometimes, it even causes medical emergencies. Moreover, breathing has its important research value in sleep hierarchy, clinical monitoring, feedback adjustments of the cardiovascular system and other fields. Therefore, monitoring and recognizing human breathing pattern is of great importance in disease diagnosis.

Traditional respiratory monitoring methods include pressure sensor, temperature sensor, respiratory inductive plethysmography (RIP) [2], etc. Recently, with the rapid development of wearable technologies, more and more wearable devices [3], which are easy to carry and can meet the individual needs of disease surveillance, have emerged in the market. Even though they are easy to carry, they still have some limitations. For patients suffering from infectious disease, skin disease and large area burn, they cannot wear contact devices. In addition, wearing wearable devices for a long time may cause skin irritation.

Non-contact monitoring can overcome these limitations to a certain extent. Non-contact monitoring methods include video, electromagnetic wave, etc. [2]. Video monitoring raises

privacy concerns and its performance is sensitive to ambient light. Biomedical radars, which monitor respiration by sending electromagnetic wave and receiving the reflected signal modulated by human chest wall movement, is less susceptible to environmental factors and has a good accuracy. It can measure the breath-induced chest wall displacement accurately [4]. Therefore, biomedical radars can be used for breathing pattern monitoring.

So far, most researches have been focused on designing the hardware and optimizing signal processing algorithms to acquire accurate measurements [5-6]. They pay attention to the monitoring of vital signs based on the biomedical radars without performing further discrimination. Lee et al [7] first used a radar to monitor different breathing patterns. They demonstrated the feasibility of Doppler radar in capturing different types of breathing patterns, without achieving the classification of breathing patterns.

Recently, machine learning has become more and more attractive in pattern recognition. Common machine learning methods [8] include SVM, k-Nearest Neighbor (KNN), Decision Tree, etc. For breathing patterns classification, different classification algorithms have been utilized in [9]. But the data were collected by wearable MEMS sensors, which still discomfort the wearer. The SVM classifier, which solves the nonlinear problem by transforming the samples into a higher dimensional space using kernel function, is a mature algorithm easy to implement [10]. It is widely used in the biomedical radar-based activity classification [11], target classification [12], etc.

In this paper, we put forward a continuous-wave (CW) Doppler radar-based automatic breathing pattern classification system using the SVM classifier. Respiration can be monitored stably and the four breathing patterns can be accurately classified. The remainder of this paper is organized as follows: Section II provides the theoretical background of Doppler radar in measuring respiration and describes four breathing patterns based on the physiological characteristics. The proposed feature extraction and machine learning method are discussed in section III. Section IV introduces the experimental setup and results. Finally, the paper is concluded in the sections V.

II. THEORY

A. Theory of Doppler Radar Breathing Detection

A 2.4-GHz digital-IF Doppler radar was employed in the experiment. It transmits a continuous single tone signal with a -7-dBm transmitting power and demodulates the return signal reflected from the chest wall of a human body. The phase information obtained after the modulation procedure is directly associated with positional change of the chest wall.

The transmitted signal can be modeled as

$$T(t) = \cos[2\pi ft + \varphi(t)] \quad (1)$$

where f is the carrier frequency and φ is the phase noise. When the chest wall is d_0 away from the radar and the chest wall displacement during the respiration is $x(t)$, the transmitted distance is $2d(t) = 2d_0 + 2x(t)$. The reflected signal is transmitted at the moment of $t - \frac{2d(t)}{c}$, where $c = \lambda f$, so the received signal can be written as

$$\begin{aligned} R(t) &= T\left[t - \frac{2d(t)}{c}\right] \\ &= \cos\left[2\pi f\left(t - \frac{2d(t)}{c}\right) + \varphi\left(t - \frac{2d(t)}{c}\right)\right] \\ &= \cos\left[2\pi ft - \frac{4\pi d_0}{\lambda} - \frac{4\pi x(t)}{\lambda} + \varphi\left(t - \frac{2d_0}{c} - \frac{2x(t)}{c}\right)\right] \end{aligned} \quad (2)$$

Because $x(t) \ll d_0$, the received signal finally can be approximated as

$$R(t) \approx \cos\left[2\pi ft - \frac{4\pi d_0}{\lambda} + \varphi\left(t - \frac{2d_0}{c}\right)\right] \quad (3)$$

In the digital-IF radar, the analog signal is directly sampled to the digital signal at an intermediate frequency (IF). In the proposed radar, the IF is 75 MHz and the sampling frequency is 100 MHz, which strictly conforms to the band pass sampling theorem [13]. Then the sampled IF signal is divided into two quadrature signals to avoid the null detection point problem, and the two quadrature signals are down-converted to the baseband quadrature signals, which can be denoted as

$$I(n) = \cos\left[\theta + \frac{4\pi x(n)}{\lambda} + \Delta\varphi(n)\right] \quad (4)$$

$$Q(n) = \sin\left[\theta + \frac{4\pi x(n)}{\lambda} + \Delta\varphi(n)\right] \quad (5)$$

where $\theta = \theta_0 + \frac{4\pi d_0}{\lambda}$ is the phase shift induced along the propagation path, $\Delta\varphi(n) = \varphi(n) - \varphi\left(n - \frac{2d_0}{c}\right)$ is the total residual phase noise, $n = 1, 2, 3, \dots, N$ is the sampling point.

The quadrature signals $I(n)$ and $Q(n)$ are combined by the arctangent operation and phase unwrapping as [14]

$$S(n) = \arctan\left[\frac{Q(n)}{I(n)}\right] + F = \theta + \frac{4\pi x(n)}{\lambda} + \Delta\varphi(n) \quad (6)$$

where F is a multiple of 180° .

Since θ and $\Delta\varphi(n)$ are nearly constant, they are removed by subtracting the average value as

$$S_0(n) = S(n) - \frac{1}{N} \sum_{n=0}^{N-1} S(n) \quad (7)$$

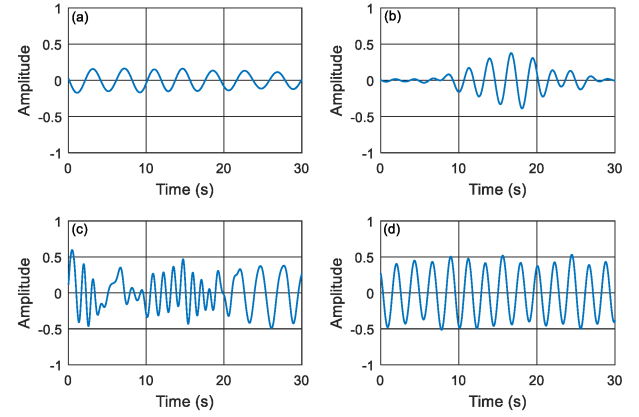


Figure 1. Four breathing patterns from Doppler radar include (a) Normal breathing (b) Cheyne-Stokes breathing (c) Dysrhythmic breathing (d) Kussmaul's breathing.

which is the final vital sign signal containing both breathing and heartbeat information. Considering the frequency range of breathing signal, a band-pass filter with cutoff frequencies 0.15 Hz and 0.7 Hz can be used to extract the breathing signal.

B. Breathing Patterns

In this section, we investigate four typical kinds of breathing patterns, which are normal breathing, Cheyne-Stokes breathing, Dysrhythmic breathing and Kussmaul's breathing. The physiological characteristics and some involved diseases of these breathing patterns will be discussed.

1) *Normal Breathing*: Generally, the rate of the normal breathing from a healthy adult is between 12 to 20 breaths per minute [7]. As shown in Figure 1(a), the subject breathes normally at a rate of approximately 15 times per minute.

2) *Cheyne-Stokes Breathing*: A breathing pattern with a cyclical crescendo-decrescendo type of sequence followed by a period of cessation is defined as Cheyne-Stokes breathing [1]. Figure 1(b) shows the time-domain waveform of Cheyne-Stokes breathing, including a period of suspended state of nearly 8s, four increasing breaths and three waning breaths. This breathing pattern is often seen in patients suffering from stroke, brain tumour, traumatic brain injury, carbon monoxide poisoning, metabolic encephalopathy, altitude sickness, narcotics use, and in non-rapid eye movement sleep of patients with congestive heart failure [1].

3) *Dysrhythmic Breathing*: Dysrhythmic breathing [7] is characterized by irregular rate and amplitude. It can be seen in Figure 1(c) that the subject breathes at an unstable rate and intensity. The breathing pattern is caused by an abnormality in the breathing patterns generator invoked in the brain stem [7].

4) *Kussmaul's Breathing*: Kussmaul's breathing [1] is the breathing pattern with increased tidal volume and frequency compared with a normal breathing. As what we can see from Figure 1(d), the subject breathes quickly and dramatically. He breathes at a rate of approximately 27 breaths per minute. This pattern is often accompanied with a severe metabolic acidosis [1].

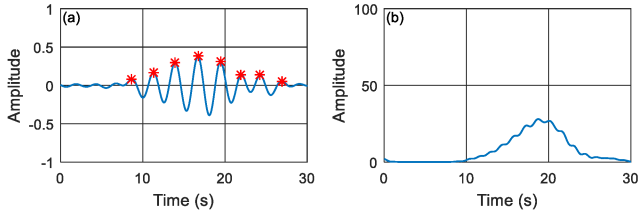


Figure 2. Feature extraction of Cheyne-Stokes Breathing: (a) the upper envelope peak (b) Short-time energy.

III. CLASSIFICATION METHOD

To classify the above mentioned four breathing patterns, three features, which are the number of peaks in the upper envelope, the minimum and variance of the short-time energy, are selected to train the classifier. The features are described in the following section. The SVM classifiers with several different kernels will be tested to classify the breathing patterns. The theory of SVM classifier will be discussed.

A. Feature Extraction

1) *The Number of Peaks in the Upper Envelope:* As shown in Figure 2, the time-domain waveforms of different breathing patterns have different upper envelope. By labeling these maximum points of the rising edge like Figure 2(a) and then calculating the number of these points, we can know the number of breaths.

2) *Minimum and Variance of Short-time Energy:* The respiration intensity in a period of time can be used to represent the short-time energy. In the four patterns that we studied, Cheyne-Stokes breathing had a short time of suspended state, which is characterized as a weak short-time energy. As shown in Figure 2(b), in the first 10 seconds of the Cheyne-Stokes breathing, the short-time energy approaches zero. Therefore, we choose the minimum short-time energy to estimate whether the breathing pattern have a period of cessation state. The variance of the short-time energy reflects breathing smoothness.

B. SVM Classifier

The support vector machine (SVM) [10, 11] is a classifier which constructs a maximal-margin hyper plane to separate the data among different classes. SVM transforms the samples into a higher dimensional space so that the nonlinear separable problem in the original sample space can be converted to linear separable problem. Raising dimension usually causes more complex calculation.

SVM ingeniously solves the problem by applying kernel function, which avoids the need to know the explicit expression of nonlinear mapping. Usually there are three kinds of kernel functions. The first kind is the linear kernel function:

$$\kappa(x_i, x_j) = x_i^T x_j \quad (8)$$

The second kind is the polynomial kernel function:

$$\kappa(x_i, x_j) = (x_i^T x_j)^d \quad (9)$$

where $d(d \geq 1)$ is the number of polynomial. When $d = 2$ or $d = 3$, the function is defined as the quadratic kernel function or the cubic kernel function, respectively.

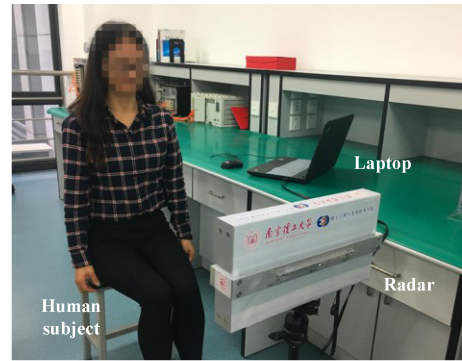


Figure 3. Experimental setup.

The last one is the Gaussian kernel function:

$$\kappa(x_i, x_j) = \exp\left(-\frac{\|x_i - x_j\|^2}{2\sigma^2}\right) \quad (10)$$

where $\sigma > 0$ is the width of the Gaussian kernel.

IV. EXPERIMENT AND ANALYSIS

This section first presents the details of the experimental setup. Then, it demonstrates the results and analyzes the data.

A. Experimental Setup

As shown in Figure 3, the subject was asked to sit on a chair facing the radar, which was placed 1m away from the subject. The height of the radar was aligned to the chest of the subject. Five healthy adults (1 female and 4 males) were selected with an average age of 23. They were trained how to perform each type of breathing before their recording sessions.

Each of them imitated every breathing pattern for three times. Therefore, there were a total of 60 data sets (5 subjects \times 4 patterns \times 3 times). Every data set is limited to 30 seconds.

B. Classification Results

We tried to classify the 60 samples using the SVM classifiers with six different kernel functions including linear, quadratic, cubic, fine Gaussian, medium Gaussian and coarse Gaussian SVMs. The Matlab Statistics and Machine Learning Toolbox were utilized for computation. The classification accuracy rates of the classifier were evaluated based on the 10-fold cross-validation [15]. In the validation, the data sets were randomly divided into ten folds. Each time, nine folds were picked up as the trained folds for the SVM classifier, and the remaining one is chosen as the test fold. This procedure was repeated for ten times and the final classification accuracy was defined as the average classification accuracy. Table I shows the classification accuracy of SVM classifiers with six different kernel functions. It can be observed the cubic SVM shows the best classification accuracy.

To further evaluate the performance of the cubic SVM classifier, the classification results for each breathing pattern are shown in Figure 4. It is shown that the cubic SVM classifier has a high classification accuracy (100%) for normal

Table I. The accuracy of SVM classifiers with six different kernel functions.

SVM Classifier	Accuracy
Linear SVM	90.0%
Quadratic SVM	85.0%
Cubic SVM	93.3%
Fine Gaussian SVM	78.3%
Medium Gaussian SVM	86.7%
Coarse Gaussian SVM	81.7%

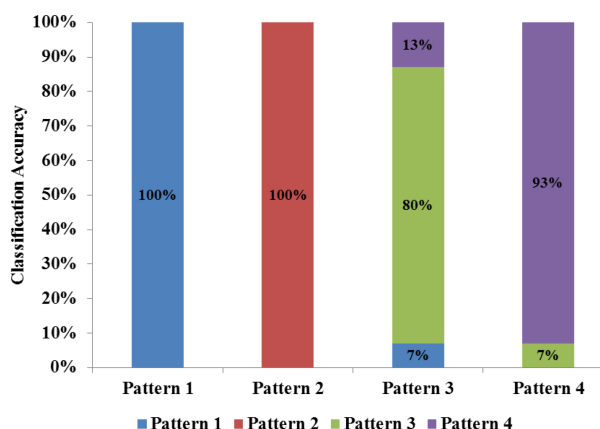


Figure 4. Classification result for each breathing pattern using the Linear SVM classifier. Pattern 1,2,3,4 refer to normal breathing, Cheyne-Stokes breathing, Dysrhythmic breathing and Kussmaul's breathing respectively.

breathing and Cheyne-Stokes breathing. The classification accuracy for Dysrhythmic breathing is 80%, but the rest 7% and 13% of Dysrhythmic breathings are misclassified as normal breathing and Kussmaul's breathing, respectively. The Kussmaul's breathing has 93% classification accuracy. While the rest 7% are mistaken as Dysrhythmic breathing. It is obvious that the main confusion is between the Dysrhythmic breathing and the Kussmaul's breathing. This is because the Dysrhythmic breathing could be mistaken as the Kussmaul's breathing featuring increased tidal volume and frequency.

V. CONCLUSION

In this paper, a continuous-wave (CW) Doppler radar-based breathing patterns classification method using SVM classifiers has been proposed. The experimental results show that the cubic SVM classifier has the best accuracy in classifying the four breathing patterns. The proposed system may be used for disease diagnosis and warning to a certain degree. In the future, more breathing patterns will be investigated and larger data sets will be constructed. The classifier could also be optimized.

ACKNOWLEDGMENT

This work was supported by the Special Foundation of China Postdoctoral Science under Grant 2013T6054, the

National Natural Science Foundation of China under Grant 61301022, the National Key Technology Support Program 2015BAI02B04, and by the Natural Science Foundation of Jiangsu Province under Grant BK20140801.

REFERENCES

- [1] G. Yuan, N. A. Drost, and R. A. McIvor, "Respiratory rate and breathing pattern," *McMaster University Medical Journal*, vol. 10, no.1, pp.23-25, Nov. 2013.
- [2] F.Q. Al-Khalidi, R. Saatchi, D. Burke H. Elphick and S. Tan, "Respiration Rate Monitoring Methods: A Review," *Pediatric Pulmonology*, vol.46, no.6,pp.523-529, Jun. 2011.
- [3] R. Ishida, Y. Yonezawa, H. Maki, H. Ogawa, I. Ninomiya, K. Sada, S. Hamada, A.W. Hahn and W.M. Caldwell, "A wearable, mobile phone-based respiration monitoring system for sleep apnea syndrome detection," *Biomedical Sciences Instrumentation*, vol 41,pp.289-293, 2005.
- [4] C. Li, Y. Xiao and J. Lin, "A 5GHz Double-Sideband Radar Sensor Chip in 0.18 μ m CMOS for Non-Contact Vital Sign Detection," in *IEEE Microwave and Wireless Components Letters*, vol. 18, no. 7, pp. 494-496, July 2008.
- [5] Y. S. Lee, P. N. Pathirana, T. Caelli and R. Evans, "Doppler radar in respiratory monitoring: Detection and analysis," *Control, Automation and Information Sciences (ICCAIS), 2013 International Conference on*, Nha Trang, 2013, pp. 224-228.
- [6] D. Zito, D. Pepe, M. Mincic, F. Zito, A. Tognetti, A. Lanata and D. De Rossi, "SoC CMOS UWB Pulse Radar Sensor for Contactless Respiratory Rate Monitoring," in *IEEE Transactions on Biomedical Circuits and Systems*, vol. 5, no. 6, pp. 503-510, Dec. 2011.
- [7] Y. S. Lee, P. N. Pathirana, C. L. Steinfort and T. Caelli, "Monitoring and Analysis of Respiratory Patterns Using Microwave Doppler Radar," in *IEEE Journal of Translational Engineering in Health and Medicine*, vol. 2, no. , pp. 1-12, 2014.
- [8] A. Khan, B. Baharudin, L.H. Lee and K. Khan, "A Review of Machine Learning Algorithms for Text-Documents Classification," *Journal of Advances in Information Technology*, vol.1, no.1, pp.4-20, Feb. 2010.
- [9] A. R. Fekr, M. Janidarmian, K. Radecka and Z. Zilic, "Respiration Disorders Classification With Informative Features for m-Health Applications," in *IEEE Journal of Biomedical and Health Informatics*, vol. 20, no. 3, pp. 733-747, May 2016.
- [10] Y. Xu, S. Zomer and R.G. Brereton, "Support Vector Machines: A Recent Method for Classification in Chemometrics," *Critical Reviews in Analytical Chemistry*, vol.36,no.3-4,pp.177-188, Mar. 2006.
- [11] Y. Kim and H. Ling, "Human Activity Classification Based on Micro-Doppler Signatures Using a Support Vector Machine," in *IEEE Transactions on Geoscience and Remote Sensing*, vol. 47, no. 5, pp. 1328-1337, May 2009.
- [12] S. Björklund, T. Johansson and H. Petersson, "Target classification in perimeter protection with a micro-Doppler radar," *2016 17th International Radar Symposium (IRS)*, Krakow, 2016, pp. 1-5.
- [13] R. Vaughan, N. Scott, and D. White, "The theory of bandpass sampling," in *IEEE Trans. Signal Process*, vol. 39, no. 9, pp. 1973-1984, Sep. 1991.
- [14] Y. Yang, C. Gu, Y. Li, R. Gale and C. Li, "Doppler Radar Motion Sensor With CMOS Digital DC-Tuning VGA and Inverter-Based Sigma-Delta Modulator," in *IEEE Transactions on Instrumentation and Measurement*, vol. 63, no. 11, pp. 2666-2674, Nov. 2014.
- [15] J. D. Rodriguez, A. Perez and J. A. Lozano, "Sensitivity Analysis of k-Fold Cross Validation in Prediction Error Estimation," in *IEEE Transactions on Pattern Analysis and Machine Intelligence*, vol. 32, no. 3, pp. 569-575, Mar. 2010.